Endothelial cell and model membranes respond to shear stress by rapidly decreasing the order of their lipid phases

Kimiko Yamamoto[1,*,‡] and Joji Ando[2,*]

[1]Laboratory of System Physiology, Department of Biomedical Engineering, Graduate School of Medicine, University of Tokyo, Tokyo 113-0033, Japan
[2]Laboratory of Biomedical Engineering, School of Medicine, Dokkyo Medical University, Tochigi 321-0293, Japan
*These authors contributed equally to this work
‡Author for correspondence (k-yamamoto@umin.ac.jp)

Accepted 22 December 2012
Journal of Cell Science 126, 1227–1234

doi: 10.1242/jcs.119628

Summary

Endothelial cells (ECs) sense shear stress and transduce blood flow information into functional responses that play important roles in vascular homeostasis and pathophysiology. A unique feature of shear-stress-sensing is the involvement of many different types of membrane-bound molecules, including receptors, ion channels and adhesion proteins, but the mechanisms remain unknown. Because cell membrane properties affect the activities of membrane-bound proteins, shear stress might activate various membrane-bound molecules by altering the physical properties of EC membranes. To determine how shear stress influences the cell membrane, cultured human pulmonary artery ECs were exposed to shear stress and examined for changes in membrane lipid order and fluidity by Laurdan two-photon imaging and FRAP measurements. Upon shear stress stimulation, the lipid order of EC membranes rapidly decreased in an intensity-dependent manner, and caveolar membrane domains changed from the liquid-ordered state to the liquid-disordered state. Notably, a similar decrease in lipid order occurred when the artificial membranes of giant unilamellar vesicles were exposed to shear stress, suggesting that this is a physical phenomenon. Membrane fluidity increased over the entire EC membranes in response to shear stress. Addition of cholesterol to ECs abolished the effects of shear stress on membrane lipid order and fluidity and markedly suppressed ATP release, which is a well-known EC response to shear stress and is involved in shear-stress Ca^{2+} signaling. These findings indicate that EC membranes directly respond to shear stress by rapidly decreasing their lipid phase order and increasing their fluidity; these changes could be linked to shear-stress-sensing and response mechanisms.

Key words: Endothelial cell, Shear stress, Caveolae, Plasma membrane, Lipid order, Membrane fluidity, Giant unilamellar vesicle

Introduction

The vascular endothelial cells (ECs) that line the inner surface of blood vessels are constantly exposed to shear stress, a mechanical force generated by flowing blood. ECs respond to shear stress by changing their morphology, functions, and gene expression, and these EC responses play important roles in maintaining the homeostasis of the circulatory system, including in controlling blood pressure, blood-flow-dependent vasodilation, and vascular remodeling (Ando and Yamamoto, 2009). Impairment of EC responses to shear stress leads to a variety of vascular diseases, including hypertension, aortic aneurysms, and atherosclerosis (Gimbrone, 1999; Yamamoto et al., 2006), however, how ECs sense shear stress as a signal and transmit it into the cell interior remains largely unknown (Davies, 1995). Previous work has revealed that shear-stress-sensing is mediated by rapid activation of various membrane molecules and microdomains, including ion channels (Gautam et al., 2006; Olesen et al., 1988; Yamamoto et al., 2000), growth factor receptors (Jin et al., 2003; Shay-Salit et al., 2002), G-protein-coupled receptors (Chachisvilis et al., 2006), caveolae (Yu et al., 2006), adhesion proteins (Osawa et al., 2002; Tzima et al., 2005), the cytoskeleton (Ingber, 1997), the glycocalyx (Florian et al., 2003), and primary cilia (Nauli et al., 2008), and these findings suggested the presence of mechanisms by which shear stress is able to activate a variety of membrane molecules and microdomains almost simultaneously. Since changes in the physical properties of the plasma membrane have been shown to affect the activity of membrane molecules (Borroni et al., 2007; Gudi et al., 1998; Phillips et al., 2009), it has been hypothesized that the EC membrane itself plays a crucial role in the mechanisms responsible for shear-stress-sensing. Although EC membrane fluidity has been demonstrated to increase under flow conditions (Butler et al., 2001; Haidekker et al., 2000), the influences that shear stress exert on the physical properties of the plasma membrane are not fully understood.

Plasma membranes are continuous bilayers of phospholipids in which various lipids and proteins are assembled. They have a dynamic, fluid structure, because most of their lipid and protein molecules are able to move about rapidly in the plane of the membrane. Plasma membranes are assumed to be in a liquid-crystalline-like state, and two distinct lipid order states are thought to coexist in the plasma membrane of each cell: a liquid-disordered state, which is characterized by loosely packed phospholipids with relatively rapid lateral diffusion, and a liquid-ordered state characterized by an aggregation of cholesterol and sphingolipids, in which the bilayer is more rigid and lipid movements are more restricted (Razani and

Lisanti, 2001). It has been possible to analyze variations in the order of the lipid phases of plasma membranes in living cells by using the environment-sensitive fluorescent probe Laurdan and two-photon microscopy (Parasassi et al., 1990; Parasassi et al., 1997). Laurdan exhibits a 50-nm red shift as the membrane lipid order changes from the liquid-ordered state to the liquid-disordered state as a result of a change in the level of water penetration into the lipid bilayer. To investigate how shear stress influences the lipid order of EC membranes, in the present study we exposed cultured ECs to controlled levels of shear stress in a flow-loading device and examined their plasma membranes for changes in Laurdan fluorescence in a real-time manner. We also examined giant unilamellar vesicles (GUVs) by Laurdan imaging to determine whether shear stress affects the lipid order of artificial lipid bilayer membranes. In addition, we studied the effects of shear stress on membrane fluidity by means of fluorescence recovery after photobleaching (FRAP) measurements (Axelrod et al., 1976).

Results

Liquid-ordered state and liquid-disordered state coexist in an EC membrane

Images of Laurdan-labeled human pulmonary artery ECs (HPAECs) were collected at different focal depths, and generalized polarization (GP) images were obtained as described in the Materials and Methods section. All GP images are shown in pseudocolor. The GP images clearly showed a heterogeneous distribution of GP values across the cell surface (Fig. 1A). It is noteworthy that high-GP regions tended to be located at the cell periphery. GP histograms exhibited two peaks, which are thought to represent liquid-ordered membrane domains (high GP values) and liquid-disordered membrane domains (low GP values) (Fig. 1B). These findings indicated that the lipid order of EC membranes is not uniform, and that in some areas it is in the liquid-ordered state while in other areas it is in the liquid-disordered state.

High-GP regions coincide with caveolar membrane domains

After the Laurdan imaging, ECs were immunostained with an antibody against caveolin-1, a marker protein for cholesterol-rich membrane microdomains called caveolae. Caveolin-1 was unevenly distributed over the cell surface and was concentrated at specific parts of the cell periphery (Fig. 1C). Comparison between the Laurdan GP images and caveolin-1 distribution revealed that the high-GP regions of the plasma membranes almost perfectly coincided with their caveolar membrane domains.

To further assess the relationships between caveolae and high-GP regions, caveolin-1 expression was knocked down with small interfering RNA (siRNA) as described previously (Yamamoto et al., 2007). Caveolin-1 knockdown with siRNA abolished the high-GP regions, while a caveolin-1 scrambled siRNA had no effect on the distribution of GP values. Treatment of ECs with methyl-β-cyclodextrin (MβCD), which disrupts caveolae by depleting plasma membrane cholesterol, significantly decreased the GP values over the entire cell membrane and abolished the high-GP regions. The effects of MβCD were prevented by cholesterol pretreatment. These findings suggested that caveolae

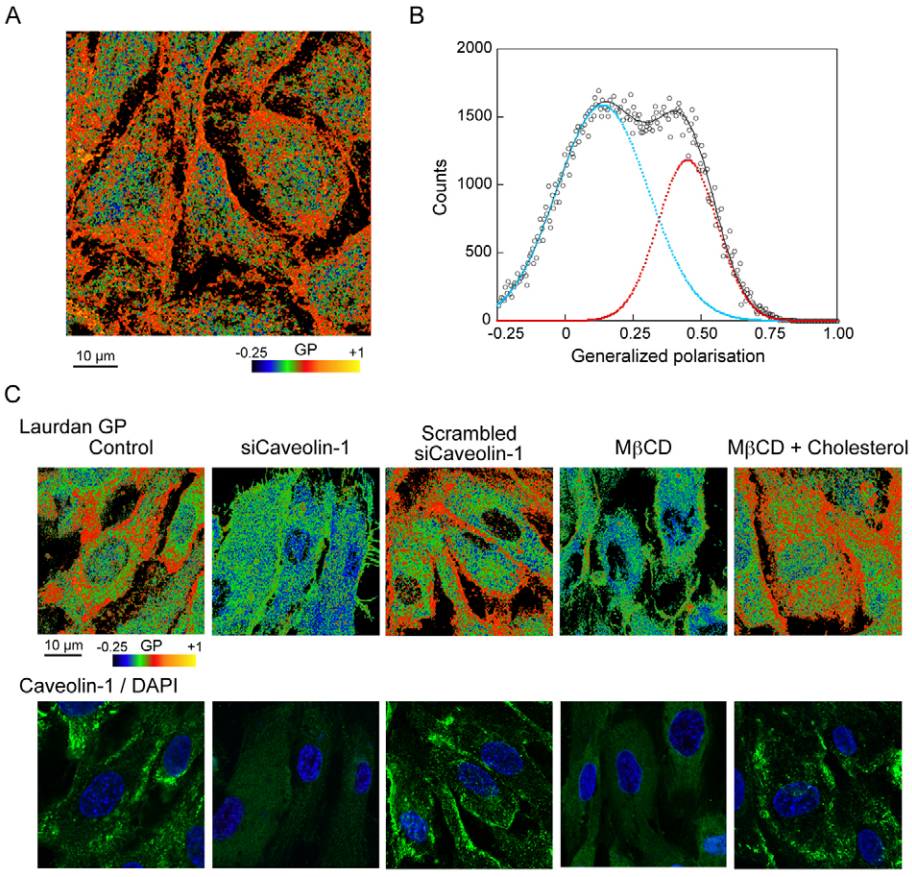

Fig. 1. Laurdan GP images of living HPAECs, GP histograms and caveolin-1 distribution. (**A**) 3D-reconstructed pseudocolored GP images, viewed from above. The colors represent different GP values according to the scale. The distribution of the GP values was broad, indicating relative heterogeneity in the lipid order of the EC membranes. Punctate high-GP regions were localized at the cell periphery. (**B**) Histogram of GP images fitted by two Gaussian distributions. The dots (black) indicate experimental data. The curve shifted to the right (red) represents liquid-ordered domains, and the curve shifted to the left (blue) represents liquid-disordered domains. (**C**) Relationship between GP values and caveolin-1 distribution. After Laurdan imaging, cells were immunostained with an antibody to caveolin-1, a marker protein for caveolae, and the cell nuclei were stained with DAPI. Control, cells cultured under static conditions; siCaveolin-1, cells transfected with a caveolin-1 siRNA; Scrambled siCaveolin-1, cells transfected with a caveolin-1 scrambled siRNA; MβCD, cells treated with 10 mM MβCD; MβCD + Cholesterol, cells treated with MβCD plus cholesterol. The high-GP regions coincided with caveolin-1-rich regions. Knockdown of caveolin-1 expression abolished the high-GP regions. The scrambled siRNA had no effect on the distribution of the GP values or caveolin-1. The high-GP, caveolin-1-rich regions disappeared after treatment with MβCD. Addition of 1.3 mM cholesterol prevented the effects of MβCD.

greatly contribute to the formation of the high-GP regions, i.e. the liquid-ordered membrane domains, in ECs.

Shear stress rapidly decreases the lipid order of plasma membranes

Laurdan-labeled HPAECs were exposed to shear stress in a flow-loading apparatus and examined for changes in membrane lipid order. As soon as shear stress was applied, GP values decreased over the entire plasma membrane, and the decrease was especially marked in the high-GP regions (Fig. 2A). The temporal changes in lipid order were quantified by placing ROIs in the high-GP regions and the low-GP regions. The GP values in both regions began to decrease immediately after the application of shear stress, continued to decrease with time, and then increased after the shear stress ceased (Fig. 2B). The GP values in the areas, where they had decreased, returned to 74.4±5.6% (means±s.d., $n=15$) of the control levels in 30 minutes. These findings indicate that EC membranes rapidly decrease their lipid order in response to shear stress, and that shear stress shifts caveolar membrane domains from the liquid-ordered state to the liquid-disordered state.

Membrane lipid order decreases dose-dependently and repeatedly in response to shear stress

When ECs were exposed to shear stress of different intensity, ranging from 5 to 20 dynes/cm^2, the GP values in the high-GP regions decreased in an intensity-dependent manner, whereas the GP values in the low-GP regions decreased in an intensity-dependent manner until reaching 10 dynes/cm^2 (Fig. 2C). The GP values of the EC membranes decreased repeatedly in response to repeated application of shear stress (Fig. 2D).

In flow-loading experiments, ECs are subjected not only to shear stress but to pressure that exerts a compressive force on the cell membrane. To determine whether the pressure affected the membrane lipid order, we applied hydrostatic pressure to ECs under no-flow conditions. The hydrostatic pressure alone had no effect on the GP values in either the high-GP or the low-GP regions, but when the same cells were exposed to shear stress, the GP values in both regions clearly decreased (Fig. 2E). This finding means that the flow-induced decrease in membrane lipid order was attributable to shear stress and not to pressure.

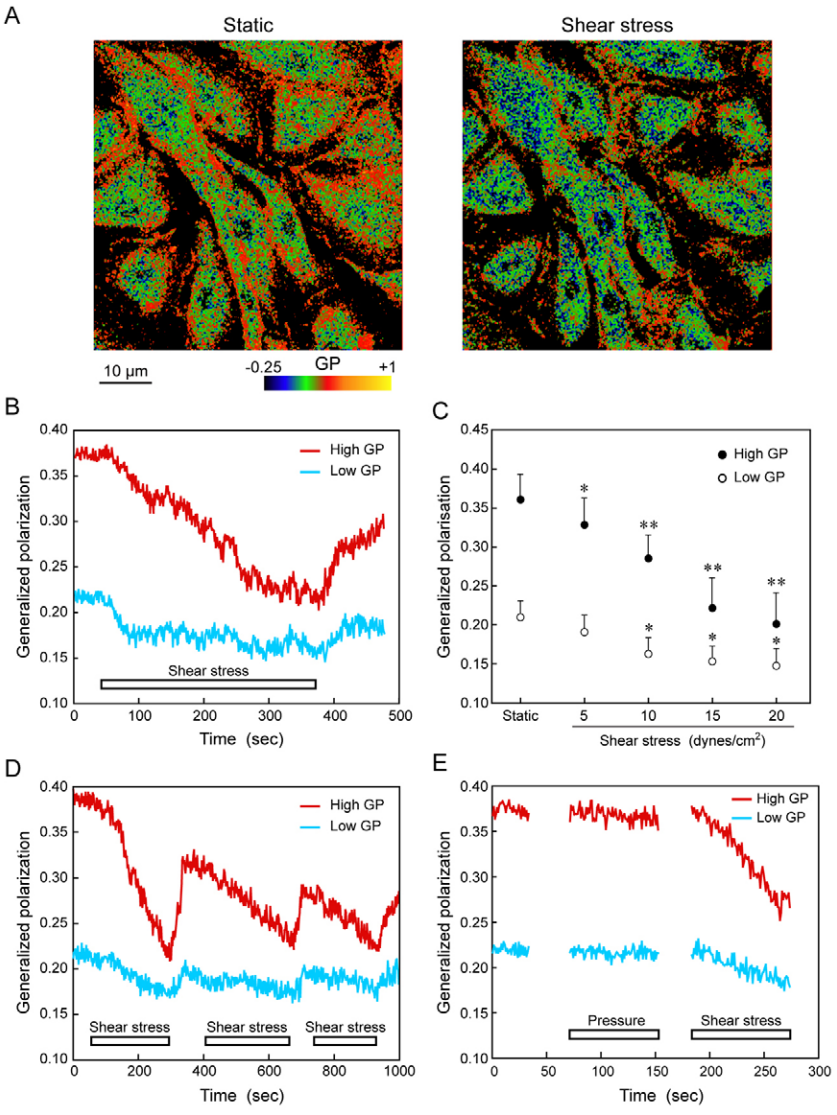

Fig. 2. Effects of shear stress on the lipid order of EC membranes. (**A**) Cross-sectional GP images before and 5 minutes after application of shear stress. Shear stress (15 dynes/cm^2) decreased GP values over the entire plasma membrane and diminished the extent of the high-GP regions localized at the cell periphery. (**B**) Temporal GP value changes in the high-GP region and the low-GP region. The GP values rapidly decreased in response to shear stress, continued to decrease with time and then increased after the cessation of shear stress. (**C**) Intensity-dependency of the shear-stress-induced changes in membrane lipid order. HPAECs were exposed to different levels of shear stress for 5 minutes and examined by Laurdan imaging. GP values in the high-GP regions decreased further as the intensity of shear stress increased. GP values in the low-GP regions decreased in an intensity-dependent manner until reaching 10 dynes/cm^2. Values are means±s.d. of 25 cells; *$P<0.05$, **$P<0.01$ compared with static control. (**D**) Ability to respond to repeated application of shear stress. Cells were subjected to repeated application of shear stress (15 dynes/cm^2) and examined by Laurdan imaging. A decrease in GP values occurred in response to each application of shear stress in both regions. (**E**) Effects of hydrostatic pressure on the membrane lipid order. Hydrostatic pressure (40 mmHg) was applied to cells under no-flow conditions but had no effect on GP values in either region. By contrast, a marked decrease in the GP values occurred in response to shear stress. Similar findings were observed in many cells.

Lipid order of artificial membranes decreases in response to shear stress

Laurdan-labeled GUVs that had attached to a poly(L-lysine)-coated coverglass were exposed to shear stress and examined for changes in the lipid order of the artificial lipid bilayer membranes. The Laurdan images and GP histograms of the GUVs showed a heterogeneous distribution of GP values across the membrane surface (Fig. 3A,B). The heterogeneity seems to be attributable to phase separation between the liquid-ordered phase and liquid-disordered phase, and the high-GP regions appear to represent lipid-ordered membrane regions, not caveolar domains. Upon shear stress stimulation, membrane lipid order decreased over the entire membrane, and the extent of the high-GP regions diminished (Fig. 3C). The temporal changes in lipid order were quantified by placing ROIs in the high-GP regions and the low-GP regions. The GP values in both regions began to decrease immediately after the application of shear stress and continued to decrease with time, and they remained at the decreased levels even after the cessation of shear stress (Fig. 3D). The data obtained from many GUVs confirmed that shear stress decreases lipid order in both high-GP and low-GP regions (Fig. 3E). These findings suggest that the lipid order response to shear stress occurs in artificial membranes as well as in the plasma membranes of living cells.

Shear stress increases membrane fluidity in ECs

Membrane fluidity is related to the mobility of membrane proteins within the lipid bilayer and has been used to assess the physical properties of plasma membranes. To investigate the effects of shear stress on membrane fluidity, FRAP measurements were made when ECs were exposed to shear stress. FRAP measurements were made after Laurdan imaging, and the cells were then immunostained with a caveolin-1 antibody (Fig. 4A). ROIs were placed in the DiI fluorescent images by referring to the Laurdan image, and ROI-1 was set in a high-GP region and ROI-2 in a low-GP region. The FRAP curves obtained under static conditions showed that fluorescence recovery in the high-GP region was significantly slower than in the low-GP region (Fig. 4B), indicating that membrane fluidity is relatively low in high-GP regions. Application of shear stress clearly accelerated fluorescence recovery in both regions. Calculation of diffusion coefficients based on the FRAP curves showed that shear stress significantly increased the membrane fluidity in both regions of the EC membranes (Fig. 4C).

We then examined how membrane-fluidity-modifying agents, such as cholesterol and benzyl alcohol, influence membrane fluidity and lipid order in HPAECs. Addition of cholesterol to ECs decreased the diffusion coefficients in both regions, whereas treatment with benzyl alcohol increased them in both regions

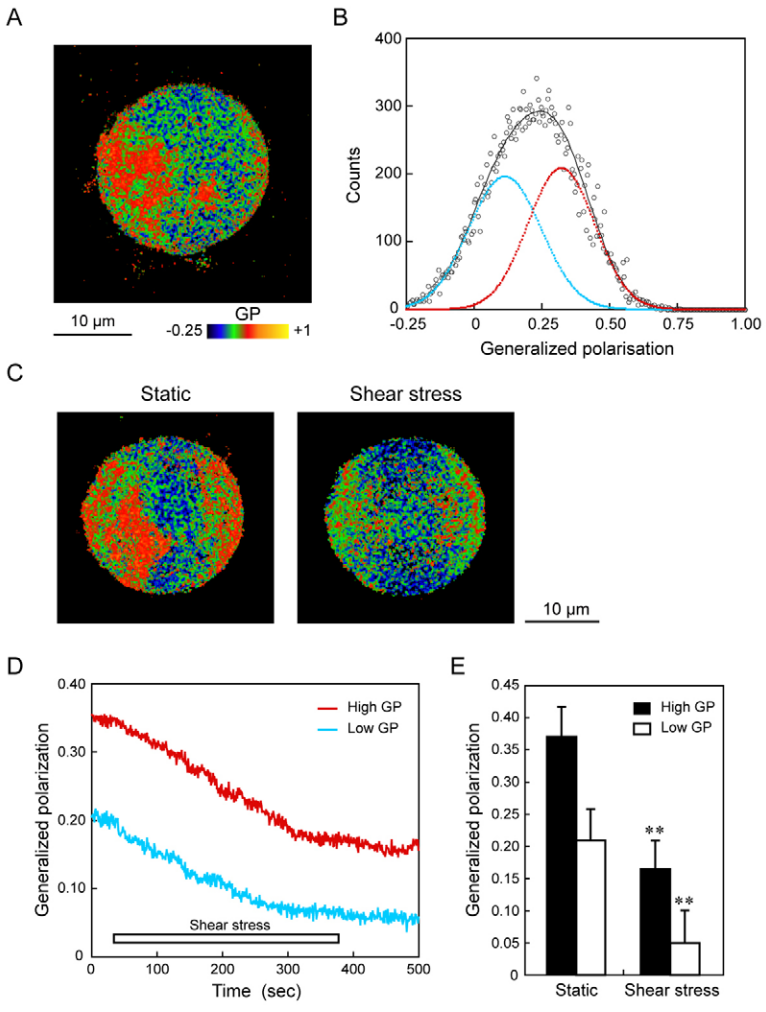

Fig. 3. Effects of shear stress on artificial lipid-bilayer membranes. (**A**) Laurdan GP image of a giant unilamellar vesicle (GUV) viewed from above. The distribution of the GP values was heterogeneous, and punctate high-GP regions were present. (**B**) Histogram of GP images fitted by two Gaussian distributions. The dots (black) indicate experimental data. The curve shifted to the right (red) represents liquid-ordered domains and the curve shifted to the left (blue) represents liquid-disordered domains. (**C**) GP images before and 5 minutes after application of shear stress. Shear stress (15 dynes/cm^2) decreased GP values over the entire membrane and diminished the extent of the high-GP regions. (**D**) Temporal GP value changes. The changes were quantified by placing regions of interest on a high-GP region and a low-GP region in a cross-sectional GP image. The GP values rapidly decreased in response to shear stress. (**E**) Quantitative analysis of the shear-induced changes in GP values. Shear stress (15 dynes/cm^2, 5 minutes) resulted in a decrease in GP values in both high-GP and low-GP regions. Values are means±s.d. of the data obtained in 12 GUVs; $^{**}P<0.01$ compared with static control.

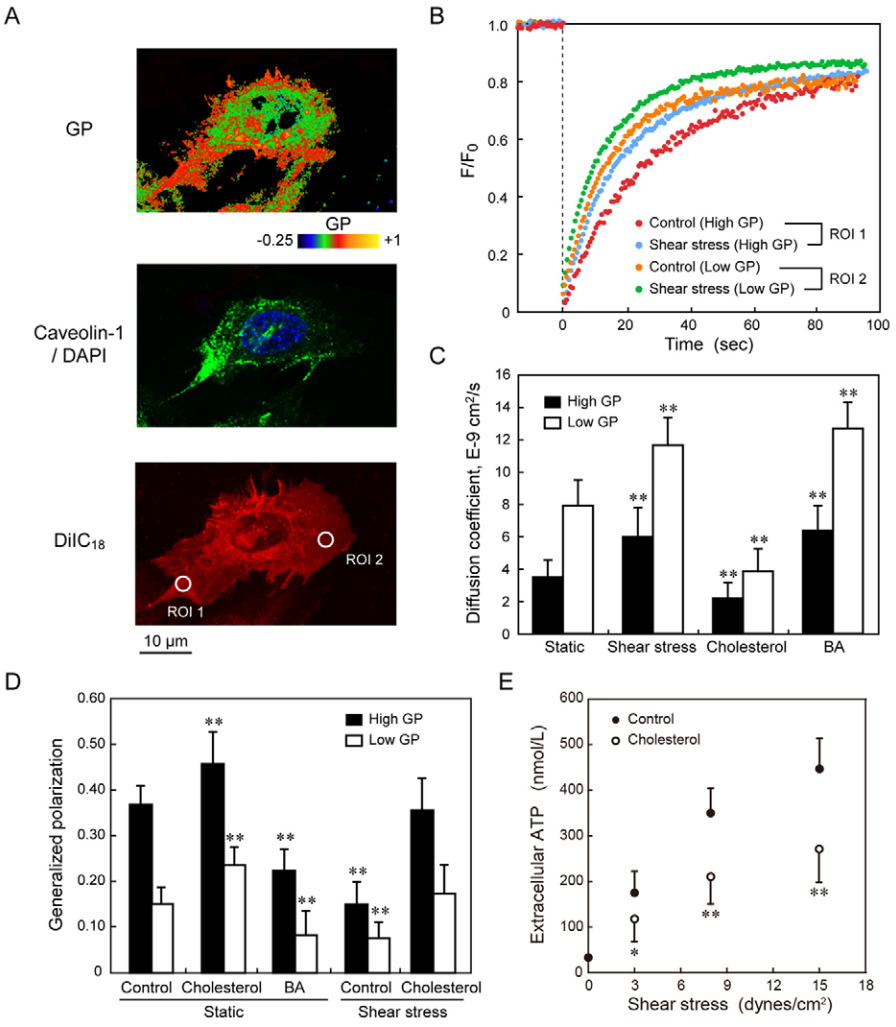

Fig. 4. Effects of shear stress on EC membrane fluidity. (**A**) Typical cell sequentially examined by Laurdan imaging, caveolin-1 immunostaining and FRAP measurements. Regions of interest were placed on the high-GP, caveolin-1-rich regions (ROI-1) and on the low-GP regions (ROI-2). (**B**) Representative FRAP curves. FRAP curves were obtained as described in the Materials and Methods section. Under static conditions, fluorescence recovery was markedly slower in ROI-1 than in ROI-2, suggesting that membrane fluidity is relatively low in high-GP regions. Application of shear stress (15 dynes/cm^2, 5 minutes) accelerated fluorescence recovery in both ROI-1 and ROI-2, indicating that shear stress increases the membrane fluidity of ECs. (**C**) Quantitative analysis of changes in membrane fluidity. FRAP measurements were performed in cells under static conditions, cells exposed to shear stress and cells treated with cholesterol (100 μM, 4 hours) or 30 mM benzyl alcohol (BA). The diffusion coefficients were based on the FRAP curves as described in the Methods and Materials section and used as a parameter of membrane fluidity. Application of shear stress resulted in an increase in the diffusion coefficient in both high-GP regions and low-GP regions. Cholesterol decreased the diffusion coefficient in both regions, whereas benzyl alcohol caused an increase. (**D**) Quantitative analysis of changes in GP values. Under static conditions, cholesterol increased the GP values in both high-GP regions and low-GP regions, whereas benzyl alcohol decreased them in both regions. Upon shear stress stimulation, the GP values significantly decreased in both regions, and cholesterol blocked the effects of shear stress. (**E**) Effects of cholesterol on shear-stress-induced ATP release. HPAECs released ATP dose-dependently in response to shear stress, and cholesterol markedly suppressed the ATP release. Values are means±s.d. of the values obtained in 20 (C,D) or 15 (E) cells; *P<0.05, **P<0.01 compared with corresponding static (C,D) or untreated (E) control.

(Fig. 4C). These findings indicated that EC membrane fluidity is sensitive to shear stress as well as to membrane-fluidity-modifying agents such as benzyl alcohol and cholesterol.

Membrane lipid order affects EC responses to shear stress

Laurdan imaging showed that the addition of cholesterol to ECs increased the membrane lipid order in both the high-GP regions and the low-GP regions under static conditions, whereas benzyl alcohol decreased it in both regions (Fig. 4D). The addition of cholesterol almost completely blocked the shear-stress-induced decrease in lipid order. To determine whether changes in the membrane lipid order influence EC responses to shear stress, HPAECs that had been treated or not treated with cholesterol were exposed to shear stress and examined for ATP release, a well-known EC response to shear stress that is involved in Ca^{2+} signaling of shear stress (Milner et al., 1990; Yamamoto et al., 2003). The amount of ATP released by ECs was measured by means of a luciferin-luciferase assay. ECs released ATP dose-dependently in response to shear stress, and the responses were markedly suppressed by treating cells with cholesterol (Fig. 4E), suggesting that the degree of membrane lipid order affects EC responses to shear stress.

Discussion

The results of the present study demonstrated that shear stress alters the physical properties of EC membranes by rapidly decreasing their lipid order. Under static conditions, the lipid order of HPAEC membranes is heterogeneous, with lipid order differing from region to region, and regions of high lipid-order being preferentially located at the cell periphery. Upon shear stress stimulation, lipid order decreased over the entire cell membrane, and the decrease was significant in the high-lipid-order regions. The lipid order responses were attributable to shear stress and not to pressure generated under flow conditions, and they were shear-stress-intensity-dependent and reversible. Interestingly, similar lipid order responses were observed in artificial lipid bilayer membranes. Application of shear stress to GUVs consisting of phospholipids and cholesterol caused a marked decrease in their membrane lipid order, indicating that the lipid order response is a physical phenomenon that does not involve participation by any membrane proteins, the cytoskeleton, or biological activities of living cells. Membrane tension induced by the application of osmotic pressure has recently been shown to induce lateral phase separation in the homogeneous membranes of GUVs which had the same

composition as our own (Hamada et al., 2011). The effects of tension and shear stress on the order of membrane lipid phases seem to be the opposite, i.e. tension increases the membrane lipid order, while shear stress decreases it. This difference may be related to the mechanisms by which cells recognize shear stress and stretching tension as different stimuli and differentially respond to each of them.

Immunostaining of HPAECs with a caveolin-1 antibody revealed that the high-lipid-order regions almost perfectly coincided with the caveolin-1-rich regions. This means that the physical property of caveolar membrane domains is different from the lipid order of other parts of plasma membranes. Similar findings have been observed in macrophages (Gaus et al., 2003). Caveolae are small flask-shaped invaginations of the plasma membrane that are rich in cholesterol and sphingolipids, and they are preferentially distributed at specific parts of the cell periphery. Because cholesterol and sphingolipids contain long, saturated fatty acids, caveolar membrane domains are in a liquid-ordered state. In addition to playing roles in endocytosis, transcytosis, cholesterol homeostasis, pathogen entry, and cancer, caveolae play crucial roles in multiple signal transduction events at the surface of various cell types (Shaul and Anderson, 1998). Research in the last decade has implicated caveolae in shear stress mechanotransduction (Park et al., 2000; Rizzo et al., 1998; Yu et al., 2006). Our previous studies demonstrated that shear stress stimulates ECs to release ATP at caveolae, and that the ATP release triggers a Ca^{2+} influx via P2X4 ion channels and subsequent propagation of Ca^{2+} waves throughout the entire cell (Yamamoto et al., 2007; Yamamoto et al., 2003). Moreover, knockdown of caveolin-1 expression with siRNA or disruption of caveolae with MβCD was found to abolish the shear-stress-induced ATP release and Ca^{2+} signaling. The results of the present study showed that caveolar membrane domains respond to shear stress by rapidly shifting from the liquid-ordered state to the liquid-disordered state. When the lipid order responses were blocked by the addition of cholesterol, ATP release by ECs in response to shear stress was markedly suppressed. Thus, it seems likely that the changes in lipid order are involved in caveola-mediated shear stress mechanotransduction.

Shear stress decreased the lipid order of EC membranes, but the mechanisms underlying the decrease remain unclear. Membrane lipid order is influenced by various factors, including changes in lipid composition, the concentration of membrane cholesterol, the density of lipid packing, relative water content, ion concentration, pH, and temperature, and shear stress may alter membrane lipid order via any of these factors or combinations of them. Studies on living cells and membrane models have shown that the cholesterol content of the membrane has a major impact on the physical properties of plasma membranes, including on their membrane fluidity (Chabanel et al., 1983; Coderch et al., 2000). In the present study, treatment of ECs with MβCD, which depletes membrane cholesterol, was found to decrease the membrane lipid order, and the addition of cholesterol prevented the effects of MβCD. Furthermore, addition of cholesterol to ECs blocked the shear-stress-induced decrease in the membrane lipid order. Thus, shear stress may alter the distribution of cholesterol in the plasma membrane or decrease its cholesterol content by incorporating cholesterol into the cytoplasm or extruding cholesterol from the cell, both of which would result in a decrease in lipid order. It is also possible that shear stress decreases membrane lipid order through changes in ion concentrations, because shear stress has been shown to increase the intracellular concentration of Ca^{2+} and protons in ECs (Yamamoto et al., 2000; Ziegelstein et al., 1992). On the other hand, shear stress may exert unknown effects on membrane lipids that lead to a decrease in lipid order. Further study is needed to clarify how shear stress decreases the lipid order of EC membranes.

In this study, Laurdan imaging and FRAP measurements were performed in the same cells. Rather than membrane fluidity being uniform over the entire cell membrane, it was found to be lower in caveolin-1-rich and high-GP regions than it was in other regions. When HPAECs were subjected to shear stress, membrane fluidity significantly increased over the entire cell membrane, and the increases in membrane fluidity were highly consistent with the findings in previous reports. When a fluorescent molecular rotor [9-(dicyanovincyl)-julolidine; DCVJ] that integrates into the cell membrane and whose quantum yield varies with membrane viscosity was used to assess membrane fluidity, the results showed that shear stress increased membrane fluidity in human umbilical vein ECs (Haidekker et al., 2000), and FRAP measurements have shown that shear stress rapidly increases membrane fluidity in bovine aortic ECs (Butler et al., 2001). Addition of cholesterol to ECs blocked the shear-stress-induced increase in fluidity and decrease in lipid order, which resulted in a significant suppression of ATP release, a rapid EC response to shear stress that is involved in Ca^{2+} signaling of shear stress (Yamamoto et al., 2003). Membrane fluidity is known to affect activities of membrane-bound proteins by influencing macromolecular interactions or by modulating conformational changes, thereby affecting cell functions (Lenaz, 1987). Therefore, changes in the physical properties of EC membranes, such as in their membrane lipid order and fluidity, especially at caveolar membrane domains, may be linked to their shear stress-sensing and response mechanisms.

Materials and Methods

Cell culture

Human pulmonary artery ECs (HPAECs) were obtained from Clonetics and grown on a 1% gelatin-coated tissue culture flask in M199 supplemented with 15% FBS, 2 mM L-glutamine (Gibco), 50 μg/ml heparin, and 30 μg/ml EC growth factor (Becton Dickinson). The cells used in the experiments conducted in this study were in the 7th and 10th passage.

Flow-loading experiments

A parallel-plate-type apparatus (FCS2, Bioptechs) was used to apply laminar shear stress to the cells, as previously described (Yamamoto et al., 2011). Briefly, the flow chamber consisted of a 1% gelatin-coated coverglass on which the cultured HPAECs rested on one side, and a glass plate on the other side, and their flat surfaces were held 200 μm apart with a Teflon™ gasket. The chamber had an entrance and an exit for the medium, and the entrance was connected to a reservoir by a silicon tube. The medium was perfused by a roller/tube pump, and the closed entire circuit was strictly kept at 37℃. [The flow chamber, the reservoir, and the connecting tube were adjusted to 37±0.2℃ by using the temperature controller (FCS2), the cord heater (CRX-4, Tokyo Giken In., Tokyo, Japan), and the polyurethane coil tube through which the water of 37℃ was perfused, respectively.] The intensity of the shear stress (τ, dynes/cm^2) acting on the EC layer was calculated by using the formula: $\tau=6\mu Q/a^2b$, where μ is the viscosity of the perfusate (poise), Q is the flow volume (ml/second), and a and b are the cross-sectional dimensions of the flow path (cm).

Preparation of giant unilamellar vesicles

GUVs were prepared essentially as described (Akashi et al., 1996; Bagatolli and Gratton, 2000). Dipalmitoylphosphatidylcholine (DPPC, Avanti Polar Lipids, Alabaster, AL), dioleoylphosphatidylcholine (DOPC, Avanti Polar Lipids), and cholesterol (Sigma) were mixed in a molar ratio of 2:2:1 in a chloroform/methanol mixture (2:1, v/v) to prepare a lipid solution that had a total lipid content of 1 mg.

Laurdan was added to the lipid solution in a Laurdan to total lipid molar ratio of 1:500. The mixtures in a 10 ml glass flask were dried with a rotary evaporator to form a thin lipid film, and the thin lipid film was subsequently dried in a vacuum for 10 hours. The thin film was then hydrated at 65℃ by introducing water-saturated N_2 gas for 20 minutes. A 5 ml volume of prewarmed >18 MΩ cm water that had been N_2 purged was gently added, and the flask was incubated at 65℃ overnight to produce GUVs. The suspension containing GUVs was slowly cooled to room temperature (23℃) over a 10-hour period. The GUVs were applied to a coverglass coated with 0.1% (w/v) poly(L-lysine) (Sigma) solution, and then were incubated for 30 minutes at room temperature to attach them to the coverglass. The GUVs were exposed to shear stress in the FCS2 chamber at 23℃ and examined by Laurdan imaging.

Laurdan two-photon microscopy

HPAECs growing on coverglasses were incubated for 30 minutes at 37℃ in culture medium containing 10 µM Laurdan dye (Molecular Probes) under a gas mixture of 95% air-5% CO_2. After rinsing the cell monolayer with HBSS, the coverglass was placed in a flow-loading apparatus and then mounted on the stage of a confocal laser-scanning microscope (TCS SP2 AOBS, Leica Microsystems, Wetzlar, Germany) equipped with a two-photon laser (MaiTai BB, Spectra-Physics). Laurdan fluorescence was excited with 770 nm wavelength light, and the emitted light was collected in the 400–460 nm range and 470–530 nm range for the two channels, respectively. General polarization (GP) was calculated by using the formula as previously described (Shentu et al., 2010):

$$\mathrm{GP} = (I_{400\text{-}460} - G \times I_{470\text{-}530})/(I_{400\text{-}460} + G \times I_{470\text{-}530}),$$

where I is light intensity, and G is a correction factor calculated through two variables: a known GP value for Laurdan in DMSO at 22℃ and the GP value of the Laurdan stock solution (500 µM) determined in each experiment. GP images (512×512 pixels) were analyzed and pseudocolored with ImageJ 1.44n software (NIH Image, National Institutes of Health, Bethesda, MD). GP distributions were obtained from the histograms of the GP images and fitted into two Gaussian distributions by using the nonlinear fitting algorithm (KaleidaGraph 4.1). GP is an indicator of the hydration depth of the bilayer interior, and it has been used to indirectly estimate changes in membrane lipid order.

FRAP measurements

HPAECs were loaded with 2.5 µM 1,1′-dihexadecyl-3,3,3′, 3′-tetramethylindocarbocyanine perchlorate ($DiIC_{18}$, Molecular Probes) for 30 minutes at 37℃ in a 95% air-5% CO_2 gas mixture. After washing the coverglass with adherent cells in HBSS, it was mounted in a flow-loading apparatus and placed on the stage of a confocal laser-scanning microscope equipped with an Ar/ArKr laser and HeNe laser (Leica). A defined region was bleached at full laser power using the 488 nm line of the laser, and a recovery of fluorescence was monitored by scanning the bleached region at low laser power (2% power at a 543 nm excitation wavelength and 555–620 nm emission wavelength). Fluorescence recovery curves were drawn by plotting the ratio (F/F_0) of fluorescence intensity during recovery from bleaching (F) to fluorescence intensity immediately after bleaching (F_0) against time, and the plots were then curve-fitted by using subroutine Origin 8 software and a theoretical equation for FRAP. Half-life time was calculated by using the formula: $t_{1/2} = -\ln(0.5)/k$ where k is a parameter obtained from the curve-fitting, and the diffusion coefficient (D) is calculated by using the formula $D = \omega^2/4t_{1/2}$, where ω is the effective radius of the focused laser beam (Yguerabide et al., 1982).

Immunohistochemistry

Cells were fixed with 4% paraformaldehyde (Sigma) and maintained in 1% normal bovine serum albumin (Sigma) to block nonspecific protein binding sites. The cells were then incubated with rabbit anti-caveolin-1 polyclonal antibody (Transduction Laboratories), and after washing they were incubated with Alexa Fluor 594 goat anti-rabbit IgG (Molecular Probes) at a 1:500 dilution. Stained cells were photographed through a confocal fluorescence microscope (Leica), and all images were imported into Adobe Photoshop as TIFFs for figure assembly.

Quantification of extracellular ATP

The ATP released by the HPAECs was measured by means of a luciferin-luciferase assay. The cells were exposed to a stepwise increase in shear stress at 37℃, and after collecting the perfusate every 20 seconds, 100-µl aliquots were applied to the ATP assay system (Toyo Ink, Tokyo, Japan). The ATP assay mixture (luciferase, D-luciferin, and bovine serum albumin) was injected into each sample, and its relative light intensity was recorded for 10 seconds in a Lumat LB 9501 luminometer (Berthold) at room temperature. A calibration curve for ATP concentrations was obtained for each experiment by using the same batch of luciferin-luciferase reagents, and the total number of moles of ATP released per second per 10^6 cells was calculated.

Statistical analysis

All results are expressed as the mean±s.d. Data were evaluated for statistical significance by an ANOVA and a Bonferonni's adjustment applied to the results of a Student's t-test performed with SPSS software. A $P<0.05$ was regarded as being statistically significant.

Acknowledgements

We wish to acknowledge Dr Akira Kamiya's invaluable support of our work, and to thank Ms Yuko Sawada for technical assistance.

Author contributions

K. Y. and J. A. designed the study, performed experiments, analyzed data, and wrote the paper.

Funding

This work was partly supported by Grants-in-Aid for Scientific from the Ministry of Education, Culture, Sports, Science and Technology Research [grant numbers S21220011 and B22300150 to J.A. and K.Y.]; and by Grants-in-Aid from the Japan Science and Technology Agency [grant number 7815 to K.Y.]; and the Canon Foundation to K.Y.

References

Akashi, K., Miyata, H., Itoh, H. and Kinosita, K., Jr (1996). Preparation of giant liposomes in physiological conditions and their characterization under an optical microscope. *Biophys. J.* **71**, 3242-3250.

Ando, J. and Yamamoto, K. (2009). Vascular mechanobiology: endothelial cell responses to fluid shear stress. *Circ. J.* **73**, 1983-1992.

Axelrod, D., Koppel, D. E., Schlessinger, J., Elson, E. and Webb, W. W. (1976). Mobility measurement by analysis of fluorescence photobleaching recovery kinetics. *Biophys. J.* **16**, 1055-1069.

Bagatolli, L. A. and Gratton, E. (2000). Two photon fluorescence microscopy of coexisting lipid domains in giant unilamellar vesicles of binary phospholipid mixtures. *Biophys. J.* **78**, 290-305.

Borroni, V., Baier, C. J., Lang, T., Bonini, I., White, M. M., Garbus, I. and Barrantes, F. J. (2007). Cholesterol depletion activates rapid internalization of submicron-sized acetylcholine receptor domains at the cell membrane. *Mol. Membr. Biol.* **24**, 1-15.

Butler, P. J., Norwich, G., Weinbaum, S. and Chien, S. (2001). Shear stress induces a time- and position-dependent increase in endothelial cell membrane fluidity. *Am. J. Physiol. Cell Physiol.* **280**, C962-C969.

Chabanel, A., Flamm, M., Sung, K. L., Lee, M. M., Schachter, D. and Chien, S. (1983). Influence of cholesterol content on red cell membrane viscoelasticity and fluidity. *Biophys. J.* **44**, 171-176.

Chachisvilis, M., Zhang, Y. L. and Frangos, J. A. (2006). G protein-coupled receptors sense fluid shear stress in endothelial cells. *Proc. Natl. Acad. Sci. USA* **103**, 15463-15468.

Coderch, L., Fonollosa, J., De Pera, M., Estelrich, J., De La Maza, A. and Parra, J. L. (2000). Influence of cholesterol on liposome fluidity by EPR. Relationship with percutaneous absorption. *J. Control. Release* **68**, 85-95.

Davies, P. F. (1995). Flow-mediated endothelial mechanotransduction. *Physiol. Rev.* **75**, 519-560.

Florian, J. A., Kosky, J. R., Ainslie, K., Pang, Z., Dull, R. O. and Tarbell, J. M. (2003). Heparan sulfate proteoglycan is a mechanosensor on endothelial cells. *Circ. Res.* **93**, e136-e142.

Gaus, K., Gratton, E., Kable, E. P., Jones, A. S., Gelissen, I., Kritharides, L. and Jessup, W. (2003). Visualizing lipid structure and raft domains in living cells with two-photon microscopy. *Proc. Natl. Acad. Sci. USA* **100**, 15554-15559.

Gautam, M., Shen, Y., Thirkill, T. L., Douglas, G. C. and Barakat, A. I. (2006). Flow-activated chloride channels in vascular endothelium. Shear stress sensitivity, desensitization dynamics, and physiological implications. *J. Biol. Chem.* **281**, 36492-36500.

Gimbrone, M. A., Jr (1999). Vascular endothelium, hemodynamic forces, and atherogenesis. *Am. J. Pathol.* **155**, 1-5.

Gudi, S., Nolan, J. P. and Frangos, J. A. (1998). Modulation of GTPase activity of G proteins by fluid shear stress and phospholipid composition. *Proc. Natl. Acad. Sci. USA* **95**, 2515-2519.

Haidekker, M. A., L'Heureux, N. and Frangos, J. A. (2000). Fluid shear stress increases membrane fluidity in endothelial cells: a study with DCVJ fluorescence. *Am. J. Physiol. Heart Circ. Physiol.* **278**, H1401-H1406.

Hamada, T., Kishimoto, Y., Nagasaki, T. and Takagi, M. (2011). Lateral phase separation in tense membranes. *Soft Matter* **7**, 9061-9068.

Ingber, D. E. (1997). Tensegrity: the architectural basis of cellular mechanotransduction. *Annu. Rev. Physiol.* **59**, 575-599.

Jin, Z. G., Ueba, H., Tanimoto, T., Lungu, A. O., Frame, M. D. and Berk, B. C. (2003). Ligand-independent activation of vascular endothelial growth factor receptor 2 by fluid shear stress regulates activation of endothelial nitric oxide synthase. *Circ. Res.* **93**, 354-363.

Lenaz, G. (1987). Lipid fluidity and membrane protein dynamics. *Biosci. Rep.* **7**, 823-837.

Milner, P., Kirkpatrick, K. A., Ralevic, V., Toothill, V., Pearson, J. and Burnstock, G. (1990). Endothelial cells cultured from human umbilical vein release ATP, substance P and acetylcholine in response to increased flow. *Proc. Biol. Sci.* **241**, 245-248.

Nauli, S. M., Kawanabe, Y., Kaminski, J. J., Pearce, W. J., Ingber, D. E. and Zhou, J. (2008). Endothelial cilia are fluid shear sensors that regulate calcium signaling and nitric oxide production through polycystin-1. *Circulation* **117**, 1161-1171.

Olesen, S. P., Clapham, D. E. and Davies, P. F. (1988). Haemodynamic shear stress activates a K^+ current in vascular endothelial cells. *Nature* **331**, 168-170.

Osawa, M., Masuda, M., Kusano, K. and Fujiwara, K. (2002). Evidence for a role of platelet endothelial cell adhesion molecule-1 in endothelial cell mechanosignal transduction: is it a mechanoresponsive molecule? *J. Cell Biol.* **158**, 773-785.

Parasassi, T., De Stasio, G., d'Ubaldo, A. and Gratton, E. (1990). Phase fluctuation in phospholipid membranes revealed by Laurdan fluorescence. *Biophys. J.* **57**, 1179-1186.

Parasassi, T., Gratton, E., Yu, W. M., Wilson, P. and Levi, M. (1997). Two-photon fluorescence microscopy of laurdan generalized polarization domains in model and natural membranes. *Biophys. J.* **72**, 2413-2429.

Park, H., Go, Y. M., Darji, R., Choi, J. W., Lisanti, M. P., Maland, M. C. and Jo, H. (2000). Caveolin-1 regulates shear stress-dependent activation of extracellular signal-regulated kinase. *Am. J. Physiol. Heart Circ. Physiol.* **278**, H1285-H1293.

Phillips, R., Ursell, T., Wiggins, P. and Sens, P. (2009). Emerging roles for lipids in shaping membrane-protein function. *Nature* **459**, 379-385.

Razani, B. and Lisanti, M. P. (2001). Caveolin-deficient mice: insights into caveolar function human disease. *J. Clin. Invest.* **108**, 1553-1561.

Rizzo, V., McIntosh, D. P., Oh, P. and Schnitzer, J. E. (1998). In situ flow activates endothelial nitric oxide synthase in luminal caveolae of endothelium with rapid caveolin dissociation and calmodulin association. *J. Biol. Chem.* **273**, 34724-34729.

Shaul, P. W. and Anderson, R. G. (1998). Role of plasmalemmal caveolae in signal transduction. *Am. J. Physiol.* **275**, L843-L851.

Shay-Salit, A., Shushy, M., Wolfovitz, E., Yahav, H., Breviario, F., Dejana, E. and Resnick, N. (2002). VEGF receptor 2 and the adherens junction as a mechanical transducer in vascular endothelial cells. *Proc. Natl. Acad. Sci. USA* **99**, 9462-9467.

Shentu, T. P., Titushkin, I., Singh, D. K., Gooch, K. J., Subbaiah, P. V., Cho, M. and Levitan, I. (2010). oxLDL-induced decrease in lipid order of membrane domains is inversely correlated with endothelial stiffness and network formation. *Am. J. Physiol. Cell Physiol.* **299**, C218-C229.

Tzima, E., Irani-Tehrani, M., Kiosses, W. B., Dejana, E., Schultz, D. A., Engelhardt, B., Cao, G., DeLisser, H. and Schwartz, M. A. (2005). A mechanosensory complex that mediates the endothelial cell response to fluid shear stress. *Nature* **437**, 426-431.

Yamamoto, K., Korenaga, R., Kamiya, A. and Ando, J. (2000). Fluid shear stress activates Ca^{2+} influx into human endothelial cells via P2X4 purinoceptors. *Circ. Res.* **87**, 385-391.

Yamamoto, K., Sokabe, T., Ohura, N., Nakatsuka, H., Kamiya, A. and Ando, J. (2003). Endogenously released ATP mediates shear stress-induced Ca^{2+} influx into pulmonary artery endothelial cells. *Am. J. Physiol. Heart Circ. Physiol.* **285**, H793-H803.

Yamamoto, K., Sokabe, T., Matsumoto, T., Yoshimura, K., Shibata, M., Ohura, N., Fukuda, T., Sato, T., Sekine, K., Kato, S. et al. (2006). Impaired flow-dependent control of vascular tone and remodeling in P2X4-deficient mice. *Nat. Med.* **12**, 133-137.

Yamamoto, K., Shimizu, N., Obi, S., Kumagaya, S., Taketani, Y., Kamiya, A. and Ando, J. (2007). Involvement of cell surface ATP synthase in flow-induced ATP release by vascular endothelial cells. *Am. J. Physiol. Heart Circ. Physiol.* **293**, H1646-H1653.

Yamamoto, K., Furuya, K., Nakamura, M., Kobatake, E., Sokabe, M. and Ando, J. (2011). Visualization of flow-induced ATP release and triggering of Ca^{2+} waves at caveolae in vascular endothelial cells. *J. Cell Sci.* **124**, 3477-3483.

Yguerabide, J., Schmidt, J. A. and Yguerabide, E. E. (1982). Lateral mobility in membranes as detected by fluorescence recovery after photobleaching. *Biophys. J.* **40**, 69-75.

Yu, J., Bergaya, S., Murata, T., Alp, I. F., Bauer, M. P., Lin, M. I., Drab, M., Kurzchalia, T. V., Stan, R. V. and Sessa, W. C. (2006). Direct evidence for the role of caveolin-1 and caveolae in mechanotransduction and remodeling of blood vessels. *J. Clin. Invest.* **116**, 1284-1291.

Ziegelstein, R. C., Cheng, L. and Capogrossi, M. C. (1992). Flow-dependent cytosolic acidification of vascular endothelial cells. *Science* **258**, 656-659.